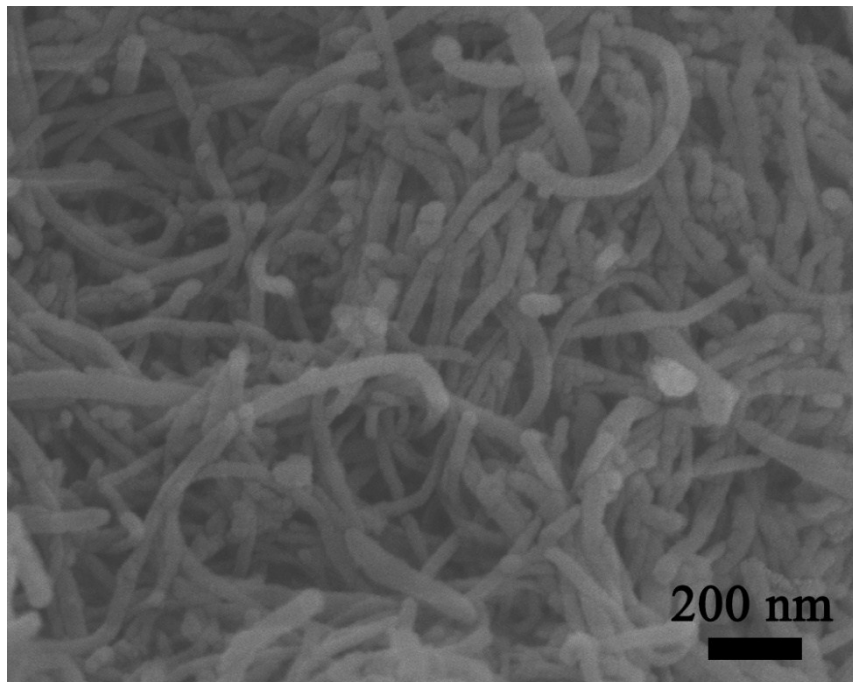


# Supporting Information

## Trace fluorinated-carbon-nanotubes induced lithium dendrite elimination for high-performance lithium–oxygen cells

Hao Cheng,<sup>a</sup> Yangjun Mao,<sup>a</sup> Yunhao Lu,<sup>b</sup> Peng Zhang,<sup>c</sup> Jian Xie<sup>\*a,d</sup> and Xinbing Zhao<sup>a,d</sup>



**Fig. S1** SEM image of the commercial fluorinated carbon nanotubes.

<sup>a</sup> State Key Laboratory of Silicon Materials, School of Materials Science and Engineering, Zhejiang University, Hangzhou 310027, P. R. China. E-mail: xiejian1977@zju.edu.cn; Fax: +86-571-87951451; Tel: +86-571-87951451

<sup>b</sup> Department of Physics, Zhejiang University, Hangzhou 310027, P. R. China

<sup>c</sup> Hangzhou Skyrich Power Co., LTD, Hangzhou 310022, P. R. China

<sup>d</sup> Key Laboratory of Advanced Materials and Applications for Batteries of Zhejiang Province, Hangzhou 310027, P. R. China

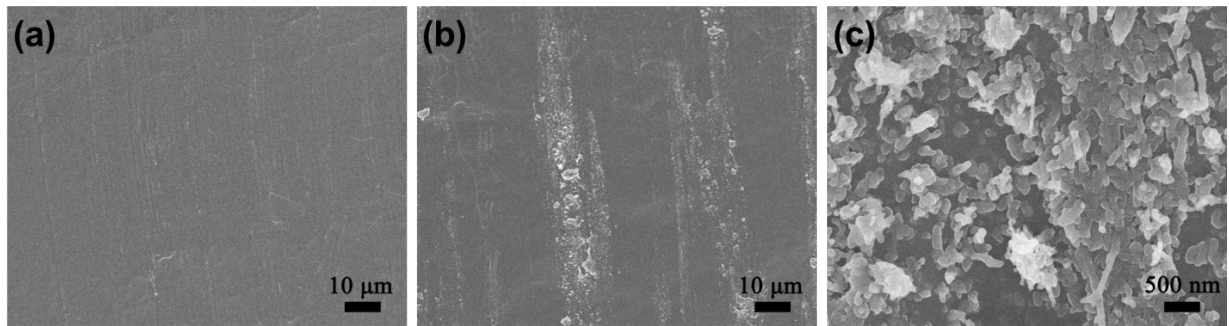


**Fig. S2** Cross-sectional SEM images of (a) bare Li and (b, c) LFCNT electrodes.

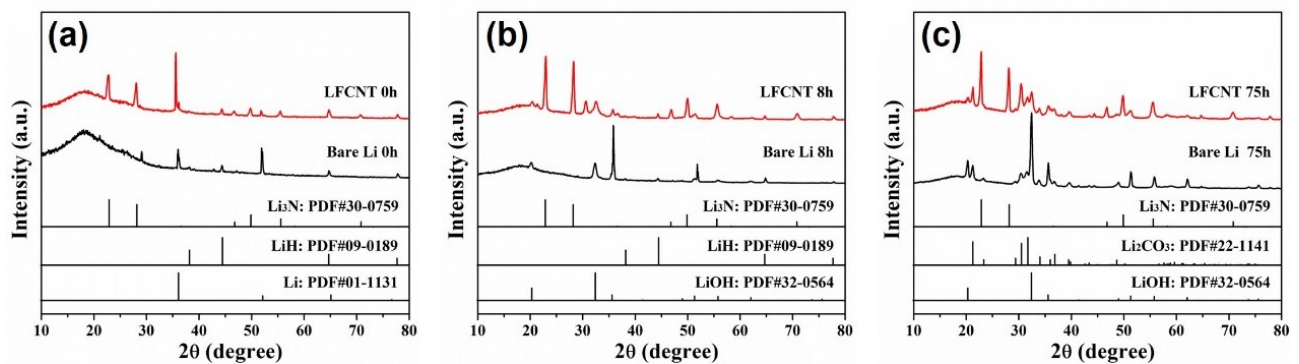


**Fig. S3** XRD patterns of LFCNT and bare Li in open air from 0 to 75 h.

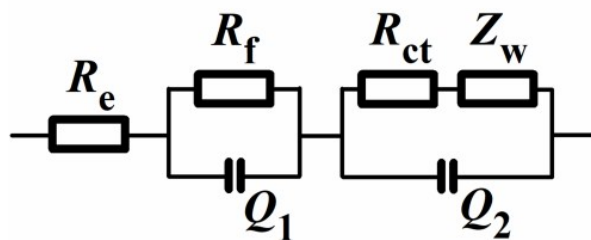


**Fig. S4** Equivalent circuit for the fitting of the electrochemical impedance, where  $R_e$  is determined by the ionic conductivity of electrolyte,  $R_f$  and  $Q_1$  correspond to the surface film resistance and relaxation capacitance,  $R_{ct}$  and  $Q_2$  correspond to the charge transfer resistance and double-layer capacitance, and  $Z_w$  is related to the bulk diffusion of Li ions.

**Table S1** Fitting results of the Nyquist plots in Fig. 2b and c using the equivalent circuit in Fig. S4.

Sample	$R_e(\Omega)$	$R_f(\Omega)$	$R_{ct}(\Omega)$	$R_{interface}(\Omega)$
LFCNT, 0 h	7.0	22.5	124.3	146.8
LFCNT, 20 h	4.8	33.9	216.9	250.8
LFCNT, 50 h	5.2	42.0	299.9	341.9
LFCNT, 100 h	9.5	49.0	349.1	398.1
LFCNT, 200 h	6.1	52.8	369.4	422.2
LFCNT, after cycling	7.9	20.2	21.0	41.2
Bare Li, 0 h	3.0	101.6	198.4	300.0
Bare Li, 20 h	3.2	188.0	272.1	460.1
Bare Li, 50 h	4.3	253.5	361.2	614.7
Bare Li, 100 h	2.6	336.9	402.2	739.1
Bare Li, 200 h	3.3	353.0	403.3	756.3
Bare Li, after cycling	3.9	32.6	48.5	81.1

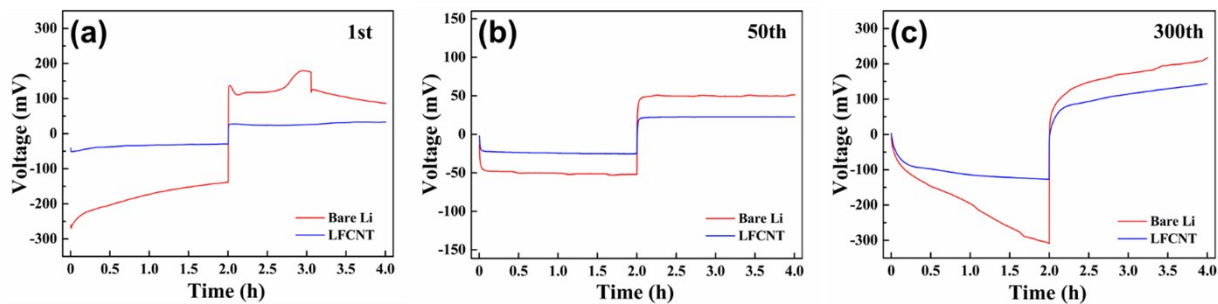


**Fig. S5** Voltage profiles of LFCNT and bare Li electrode in symmetric cells at  $0.5 \text{ mA cm}^{-2}$  with a capacity of  $1 \text{ mAh cm}^{-2}$  in the (a) 1st cycle, (b) 50th cycle, and (c) 300th cycle.

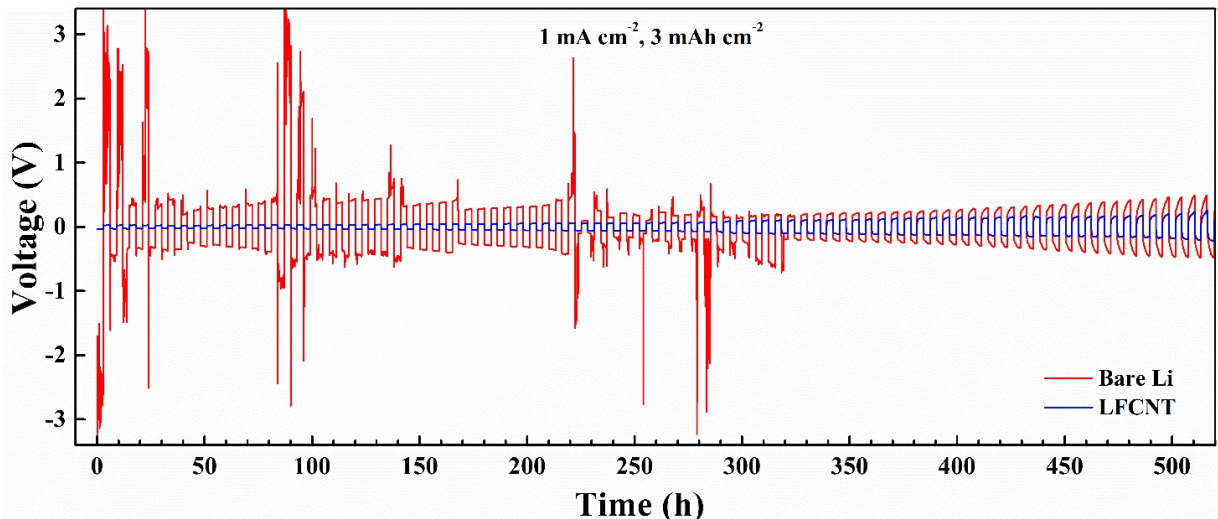


**Fig. S6** Galvanostatic discharge/charge profiles of LFCNT and bare Li electrodes in symmetric cells at  $1 \text{ mA cm}^{-2}$  with a capacity of  $3 \text{ mAh cm}^{-2}$ .

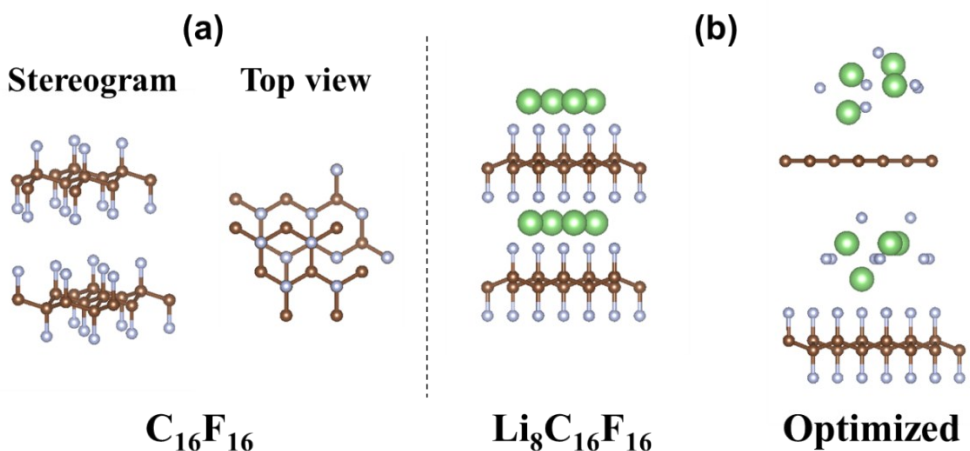


**Fig. S7** (a) Model of the bilayer fluorinated graphene, and (b) the corresponding side view of Fig. 4g.

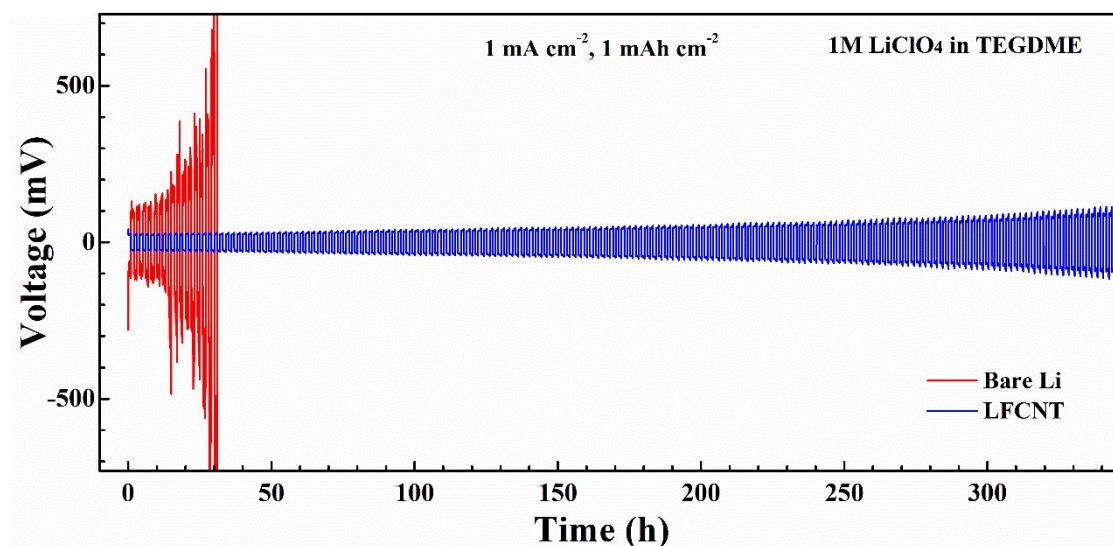


**Fig. S8** Galvanostatic discharge/charge profiles of LFCNT and bare Li electrodes in symmetric cells based on 1 M LiClO<sub>4</sub>/TEGDME tested in O<sub>2</sub> atmosphere at 1 mA cm<sup>-2</sup> with a capacity of 1 mAh cm<sup>-2</sup>.

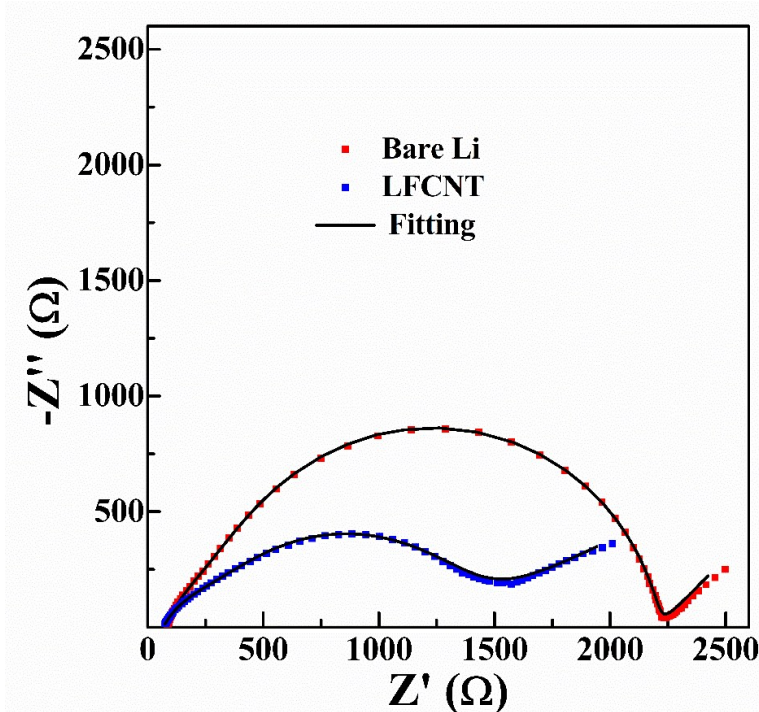


**Fig. S9** Nyquist plots of the Li–O<sub>2</sub> cells with bare Li and LFCNT electrode.

**Table S2** Fitting results of the Nyquist plots in Fig. S9 using the equivalent circuit in Fig. S4.

Sample	$R_e(\Omega)$	$R_f(\Omega)$	$\frac{Q_1}{Y}$		$R_{ct}(\Omega)$	$\frac{Q_2}{Y}$	
			$n$	$Q_1$		$n$	$Q_2$
Cell with bare Li	83.4	243.5	4.6×10 <sup>-6</sup>	0.79	1878.0	2.3×10 <sup>-6</sup>	0.92
Cell with LFCNT	68.3	241.0	5.7×10 <sup>-6</sup>	0.72	932.0	1.3×10 <sup>-5</sup>	0.77

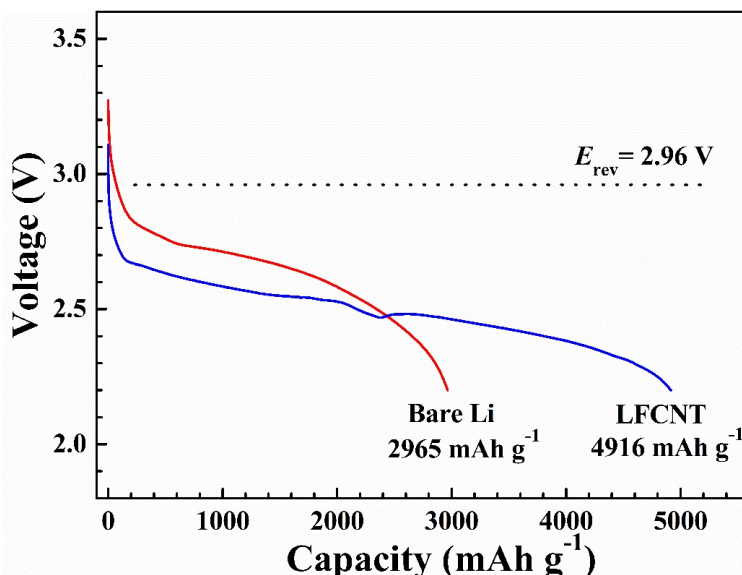


**Fig. S10** Discharge profiles of Li–O<sub>2</sub> cells with bare Li and LFCNT electrode at 100 mA g<sup>-1</sup>.

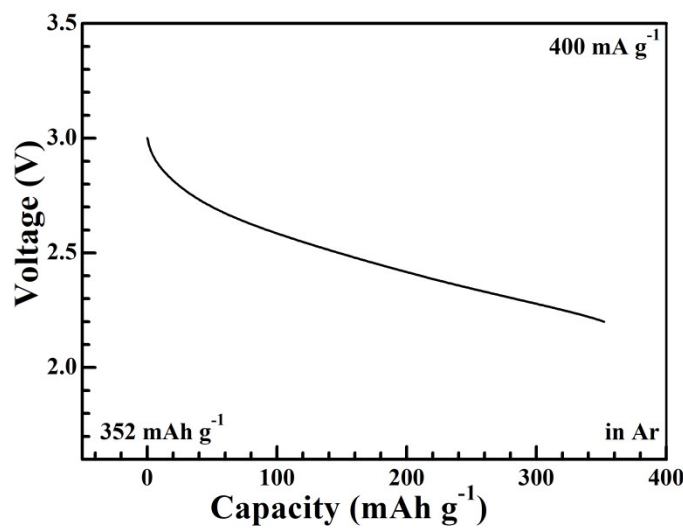


**Fig. S11** Discharge profile of Li/MnO<sub>2</sub> cell in pure Ar.

**Table S3** Comparison of electrochemical performance of Li–O<sub>2</sub> cells with various Li anodes.

Cathode	Anode	Current density	Specific capacity	Cycle number	Reference
<b>δ-MnO<sub>2</sub></b>	<b>LFCNT</b>	<b>400 mA g<sup>-1</sup> (0.2 mA cm<sup>-2</sup>)</b>	<b>1000 mAh g<sup>-1</sup></b>	<b>135</b>	<b>This work</b>
Ketjen black carbon	Li stabilized by LiTNFSI	500 mA g <sup>-1</sup>	500 mAh g <sup>-1</sup>	49	[1]
Ketjen black carbon	phosphorene-coated Li	250 mA g <sup>-1</sup>	1000 mAh g <sup>-1</sup>	50	[2]
CNT-Based Air Electrode	Li with highly concentrated electrolyte	0.1 mA cm <sup>-2</sup>	1000 mAh g <sup>-1</sup>	55	[3]
MWCNTs electrode	CPL-Coated Li	250 mA g <sup>-1</sup>	1000 mAh g <sup>-1</sup>	60	[4]
Ketjen black carbon	DOA-treated Li	100 mA g <sup>-1</sup>	500 mAh g <sup>-1</sup>	65	[5]
CNT-based air electrode	Li stabilized by highly-concentrated electrolyte	0.1 mA cm <sup>-2</sup>	600 mAh g <sup>-1</sup>	90	[6]
Porous graphene cathode	porous graphene/Li anode.	1000 mA g <sup>-1</sup>	1000 mAh g <sup>-1</sup>	100	[7]
Super P	FEC-treated Li	300 mA g <sup>-1</sup>	1000 mAh g <sup>-1</sup>	106	[8]

## References

- 1 B. Tong, J. Huang, Z. B. Zhou and Z. Q. Peng, *Adv. Mater.*, 2017, **30**, 1704841.
- 2 Y. J. Kim, D. Koo, S. Ha, S. C. Jung, T. Yim, H. Kim, S. K. Oh, D. M. Kim, A. Choi, Y. Kang, K. H. Ryu, M. Jang, Y. K. Han, S. M. Oh and K. T. Lee, *ACS Nano*, 2018, **12**, 4419–4430.
- 3 B. Liu, W. Xu, P. F. Yan, X. L. Sun, M. E. Bowden, J. Read, J. F. Qian, D. H. Mei, C. M. Wang and J. G. Zhang, *Adv. Funct. Mater.*, 2016, **26**, 605–613.
- 4 D. J. Lee, H. Lee, Y. J. Kim, J. K. Park and H. T. Kim, *Adv. Mater.*, 2016, **28**, 857–863.
- 5 X. Zhang, Q. M. Zhang, X. G. Wang, C. Y. Wang, Y. N. Chen, Z. J. Xie and Z. Zhou, *Angew. Chem. Int. Ed.*, 2018, **57**, 12814 –12818.
- 6 B. Liu, W. Xu, P. F. Yan, S. T. Kim, M. H. Engelhard, X. L. Sun, D. H. Mei, J. Cho, C. M. Wang and J. G. Zhang, *Adv. Energy Mater.*, 2017, **7**, 1602605.
- 7 G. Huang, J. H. Han, C. C. Yang, Z. Q. Wang, T. Fujita, A. Hirata and M. W. Chen, *NPG Asia Mater.*, 2018, **10**, 1037–1045.
- 8 Q. C. Liu, J. J. Xu, S. Yuan, Z. W. Chang, D. Xu, Y. B. Yin, L. Li, H. X. Zhong, Y. S. Jiang, J. M. Yan and X. B. Zhang, *Adv. Mater.*, 2015, **27**, 5241–5247.

## **Information for videos**

**Video 1** Dynamic changes of the LFCNT electrode at  $1 \text{ mA cm}^{-2}$  without separator.

**Video 2** Dynamic changes of the bare Li electrode at  $1 \text{ mA cm}^{-2}$  without separator.

**Video 3** Dynamic changes of the LFCNT electrode at  $1 \text{ mA cm}^{-2}$  with separator.

**Video 4** Dynamic changes of the bare Li electrode at  $1 \text{ mA cm}^{-2}$  with separator.